European Journal of Radiology 131 (2020) 109261

Contents lists available at ScienceDirect

European Journal of Radiology

journal homepage: www.elsevier.com/locate/ejrad

Review

Technological developments of X-ray computed tomography over half a century: User's influence on protocol optimization

Ronald Booij *, Ricardo P.J. Budde, Marcel L. Dijkshoorn, Marcel van Straten

Department of Radiology & Nuclear Medicine, Erasmus MC, Rotterdam, P.O. Box 2240, 3000 CA, The Netherlands

ARTICLE INFO

Keywords:
Computed x ray tomography (MeSH)
Health physics
Radiation dosage
Diagnostic imaging

ABSTRACT

Since the introduction of Computed Tomography (CT), technological improvements have been impressive. At the same time, the number of adjustable acquisition and reconstruction parameters has increased substantially. Overall, these developments led to improved image quality at a reduced radiation dose. However, many parameters are interrelated and part of automated algorithms. This makes it more complicated to adjust them individually and more difficult to comprehend their influence on CT protocol adjustments. Moreover, the user's influence in adapting protocol parameters is sometimes limited by the manufacturer's policy or the user's knowledge. As a consequence, optimization can be a challenge. A literature search in Embase, Medline, Cochrane, and Web of Science was performed. The literature was reviewed with the objective to collect information regarding technological developments in CT over the past five decades and the role of the associated acquisition and reconstruction parameters in the optimization process.

1. Introduction

Computed tomography (CT) has fundamentally changed the practice of medicine and continues to expand our knowledge about diseases and management of major health challenges [1]. Consequently, the number of CT scans performed worldwide is constantly increasing. The number of CT exams obtained per year in the United States was around 3 million at the early eighties, increasing with approximately a factor of 20–62 million performed CT exams in 2007 [2]. The rapid increase of CT use was seen in European countries as well, and where previously CT scans of mainly adults were performed, there is an increase of CT's performed in pediatric patients [3,4]. Especially the latter are believed to benefit from technological innovations such as high-speed CT scanning that improve diagnostic capabilities in these patients. But, just like in adults, these scans should always be justified [2,5]. Without a doubt, CT scanning is the biggest contributor of radiation exposure to the collective effective dose of medical examinations worldwide [3,6]. Dutch researchers found that the increase in CT exams was not primarily due to the growth and aging of the Dutch population, but can be explained by its easy accessibility, associated technological developments and capabilities. In parallel with the increase of performed CT scans, public awareness and concerns about medical radiation exposure increased [7,8]. The radiology community is aware of this fear and technological developments for radiation dose optimization have always been at their attention. However, optimization of a scanning protocol with respect to image quality (IQ) and radiation dose is a delicate procedure, mainly due to the interrelation of parameters. Furthermore, system properties and accompanying data acquisition techniques changed and expanded over the years. In this paper, we present an overview of the technological developments during the evolution of CT and the accompanying user's influence for protocol optimization. Finally, a future outlook on technological developments is given.

2. Search strategy

Embase, Medline, Cochrane, and Web of Science were used for the literature search for this narrative review by combining synonyms for 'image quality', 'radiation dose', and 'CT' with English language

Abbreviations: AEC, automatic exposure control; AI, artificial intelligence; ATCM, automated tube current modulation; CNR, contrast-to-noise ratio; CT, computed tomography; DSCT, dual source computed tomography; ECG, electrocardiogram; FBP, filtered backprojection; FoV, field of view; IQ, image quality; IR, iterative reconstruction; kVp, peak kilovolt; MDCT, multi-detector CT; PCCT, photon counting CT; TR, temporal resolution.

* Corresponding author.
E-mail addresses: r.booij@erasmusmc.nl (R. Booij), r.budde@erasmusmc.nl (R.P.J. Budde), m.l.dijkshoorn@erasmusmc.nl (M.L. Dijkshoorn), marcel.vanstraten@erasmusmc.nl (M. van Straten).

https://doi.org/10.1016/j.ejrad.2020.109261
Received 16 March 2020; Received in revised form 11 August 2020; Accepted 27 August 2020
Available online 31 August 2020

restriction. The full search syntax is provided in the Appendix A of the supplementary material. Duplicates were removed and reference lists of included articles and review articles were searched for additional articles. First, articles were screened on title and abstract. Non-original research articles, e.g. case-reports, and original research articles not containing information on image quality and radiation dose regarding CT were excluded. Inclusion, exclusion, and screening of all articles was performed by one author (RBo). Selection criteria were articles containing information regarding key technological developments in CT and the accompanied influence of those developments on image quality and/or radiation dose. After the search, we continued to prospectively add recent articles of which we thought that they supported the text.

3. System properties

The user's influence and choices in protocol optimization depend on the CT scanner's technological capabilities and system properties. Main technological developments of system properties, acquisition, and reconstruction parameters are presented in Table 1 and are discussed below. An overview of the evolution of CT scanners and the technical advances in CT, is illustrated in Fig. 1.

3.1. Translation-rotation and slip ring technology

Initially, CT images were acquired by the translation-rotation method in the "first and second" generation CT scanners. Within this method, data was acquired by the x-ray tube and detector moving in a linear translatory pathway and was repeated with small rotational increments [9]. The third generation CT scanners have a wide fan beam and detectors that rotated slowly around the patient, requiring multiple breath holds to complete an axial CT exam. There was a high chance in missing abnormalities due to the multiple breath holds (Fig. 1a). Slip ring technology introduced in 1987 allowed continuous rotation of the tube and detectors by transferring electrical energy to the rotating gantry part and transmission of measured data to the computer system [10]. As the fourth generation scanners, with a stationary detector ring, did not get widely accepted, all currently available CT scanners are third generation scanners by design. Therefore, we will only briefly comment on special scanner concepts like electron beam CT and dynamic spatial reconstructor.

3.2. Detectors

The total beam collimation in the longitudinal, or z-direction, in the first-generation CT scanners was limited to one detector of 8–13 mm in width, but detector size decreased rapidly to 2–8 mm [11,12]. With the introduction of spiral multi-detector CT (MDCT) in 1998 (also known as multi-slice CT), the individual detector elements became even smaller, down to 0.25 mm per detector element nowadays [13], resulting in improved spatial resolution. Moreover, it provided more and fast longitudinal coverage since multiple detector elements were combined (Fig. 1) [14]. Currently, for several CT manufacturers the total beam collimation is up to 160 mm with multiple detectors in the z-direction, allowing dynamic data acquisition of e.g. the entire brain or heart without table movement [15,16]. Another positive outcome of an increased total collimation, is the decrease of the overbeaming effect: The collimated x-ray beam is always wider than the total detector width because of the penumbra, which does not contribute to the image reconstruction, but does increase radiation dose. Although the impact of overbeaming on radiation dose was reduced with increased total collimation, overranging dose increases with increasing collimation and pitch values [17]. Therefore, a dynamic collimator was introduced in 2009 to reduce the amount of pre- and post-spiral dose which are irrelevant for image reconstruction and is automatically applied [18].

Another approach to detector developments were improved detector efficiency to increase radiation dose efficacy, and the introduction of dual layer detectors. These detectors can measure x-ray attenuation for low and high energy photons separately in two different detector layers, enabling material identification and quantification [19].

3.3. X-ray tube

With the introduction of spiral CT, the x-ray tubes had to be redesigned again to cope with overheating problems because of the need for increased tube output [20]. The introduction of a periodic motion of the focal spot in the z-direction resulted in doubling measurement positions in the longitudinal direction per rotation; thereby increasing spatial resolution and eliminating aliasing artifacts [21]. This multifan measurement technique is commonly known as z-flying focal spot and "double-dynamic" focus and applied by several vendors

Recent developments also include an additional tin filtration within the x-ray tube, which is of particular use in e.g. unenhanced CT high contrast studies of the chest and sinus [22,23] and is currently applied by one vendor.

3.4. Dual source CT (DSCT)

CT scanners with multiple x-ray sources can provide fast imaging and improved temporal resolution (TR). The dynamic spatial reconstructor was one of the first attempts to introduce such a CT system but was never

Table 1
Timeline Main Technological Developments of System Properties, Acquisition, and Reconstruction Parameters over the Course of Half a Century of Computed Tomography.

Decades	\`70 s - \`80s		\`90s		\`00s		\`10s	
System properties	Gas detectors	Fan beam	Solid state detectors	Detector collimation	Dual source CT	Dynamic collimation	Electronic noise	Additional tin filtration
	Translation-rotation	Slip ring			Wide area CT			
Acquisition properties	Constant tube voltage	Rapid tube voltage switching dual energy	ECG-pulsing	Automated tube current modulation	Temporal resolution	Dual energy	Automatic tube voltage selection	
	Constant tube current				ECG-guided dose modulation	4DCT	Routinely low tube voltage	
	Sequential scanning	ECG-gating	Spiral scanning	Multi-detector spiral				
Reconstruction properties	Algebraic reconstruction	180- and 360-degree reconstruction	Reconstruction speed	Slice thickness	Noise & motion reduction	Temporal resolution	Increased matrix size	Artificial intelligence
	Filtered back-projection						Iterative reconstruction	Advanced beam hardening correction

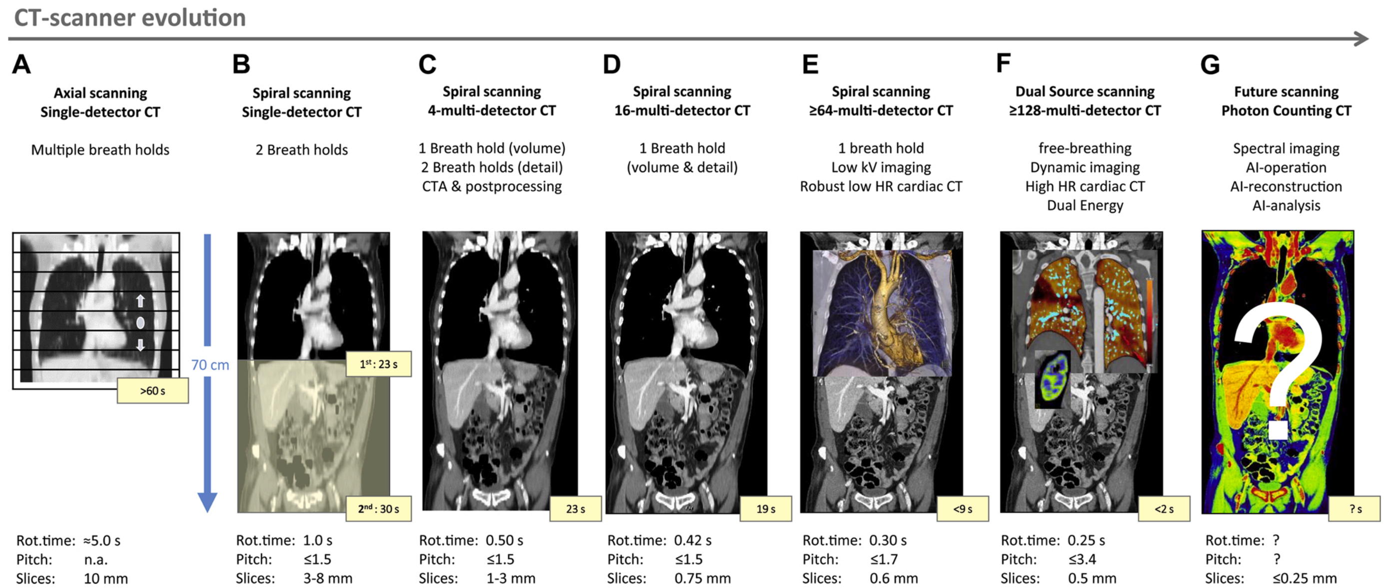

Fig. 1. (a-g) Graphical representation of the evolution of third-generation CT scanner technology from a single detector row design to expected future technology. The coronal multiplanar reconstructions (MPR) of the thorax-abdomen that illustrate the improvements of MPR quality over time, are based on a dataset of one patient (at one moment in time). **(a)** Single-detector (row) 10 mm axial scan. **(b)** Spiral single-detector scan needed at least two breath holds for a full thorax-abdomen scan. **(c)** Multi-detector CT. **(d)** Spiral CT with 16 detector rows allowed for volume scanning with isotropic datasets. **(e)** Faster rotation times and 64-detector CT allowed for robust cardiac CT exams. **(f)** Free-breathing and dual energy possibilities with dual source CT. **(g)** Future technologies. The color scale is used for illustrative purposes only and does not reflect true photon counting (PCCT) or spectral CT.
See text for more details.

used in clinical routine [24]. In 2005, the first DSCT with two tubes and two corresponding detectors was introduced, demonstrating improved TR and dual energy imaging capabilities in clinical practice which was widely accepted [25].

4. Acquisition parameters

The main developments in acquisition parameters and how they influence image acquisition are discussed next.

4.1. Tube current

Within the first-generation CT scanners, the user could set tube current (mA value) depending on the accompanying tube voltage [26,27]. Tube current was constant during a scan and this remained so for almost twenty years.

4.2. Automated tube current modulation (ATCM)

ATCM was introduced end ’90 s as part of the automatic exposure control (AEC) [28]. Early strategies consisted of online angular tube current modulation only, where nowadays it is often applied in combination with tube current adaptation in longitudinal directions. Some strategies enabled users to set customizable quality levels to achieve a constant noise level, whereby tube current is adjusted for the chosen scan and reconstruction parameters. Algorithms within the latest systems may suggest adjustments to average tube current and image noise based on a user defined dose index and patient diameter, accounting for the use of iterative reconstructions (IR) and used tube voltage. Another strategy was to have the ATCM system measure the attenuation from patients in a specific protocol, using this as a standard protocol body attenuation. The user can determine a noise reference or set the tube current to individual patient habitus. A different approach of fully ATCM is adaptation to different anatomical regions and patient sizes by setting a target tube current level for a standard-size reference patient [29]. The user may set different tube current modulation schemes for different patient sizes and anatomical regions.

A high level of awareness by the users for optimal positioning of the patient in the CT scanners is of utmost importance [30,31]. Both radiation dose and IQ may be affected when the CT localizer radiograph, which is used by the AEC, is made with the patient positioned off-center [30,31].

4.3. Tube voltage

Within the first and second generation CT scanners, the user was able to set the peak tube voltage in the range of 100–140 kilovolt peak (kVp) [27,32,33]. These high voltages are much appreciated when imaging thick patients, or to reduce metal implant artifacts, however radiation dose is likely to be increased. Lowering the tube voltage requires tube current to be increased, and this was often limited by tube power early on.

4.4. Automatic tube voltage selection

Changing the tube voltage in predefined scan protocols, requires understanding of its influence on signal-to-noise ratio and contrast-to-noise ratio (CNR). Therefore, it could be challenging for users to understand how to perceive an improved IQ, or even the same IQ while reducing radiation dose, when changing the tube voltage. It was until the ’10 s that integrated automatic tube voltage selection and accompanying tube current adjustment became fully integrated into the AEC. Currently, it is available in most CT systems [34]. The main goal of automated tube voltage selection is to control the CNR and thereby minimize radiation dose. The user can define settings for the anatomical region and exam type with or without contrast.

4.5. Dual energy imaging

Dual energy, or so-called spectral imaging, can add tissue information to the CT image (e.g. discriminate bone from iodine-enhanced tissue). The possibility of determining the atomic number of the materials within a slice was already discussed by Sir Hounsfield in the seventies [12]. First attempts were done by a double scan: once with a high tube voltage and once with a low tube voltage and in parallel by a rapid kV switching technique. However, clinical use was rather limited due to needed technological improvements and high costs. The introduction of DSCT in 2005 allowed the acquisition of nearly simultaneous dual-energy data by using two tubes (Fig. 1f) [35]. A few years later, this was also made possible with the introduction of an improved rapid tube voltage switching technique [36]. TwinBeam CT and Dual layer spectral CT are the latest technologies to acquire dual energy datasets [19,37].

4.6. Scan mode

4.6.1. Sequential scanning

Sequential CT imaging represents scanning with a stationary scanner table while the x-ray tube is rotated around the patient. After the scan, the patient is transported with a predefined incremental step. Then the next acquisition is performed and the process is repeated to the end of the scan range.

4.6.2. Spiral scanning

CT entered a new era with spiral CT (also known as helical scanning) in the late 1980s [38,39]. The scanner table was able to travel at a constant speed through the gantry, i.e. the table feed, with the tube rotating, allowing the acquisition of volumetric data. It also introduced the concept of pitch (the ratio between the table feed per full rotation and total beam collimation) which can be adjusted by the user. With single-detector spiral CT and a reduced rotation time, scan time was reduced. However, scans were restricted to single organs. A complete thorax-abdomen scan required at least two breath holds (Fig. 1b). The introduction of MDCT (Fig. 1c) gave the user the choice to scan with a small detector row width (e.g. 4×1 mm) to increase spatial resolution (=detail) or to scan with a large detector size, e.g. 4×2.5 mm, to reduce scan time (=volume). Spiral scanning with a 16-row MDCT allowed isotropic datasets of large volumes and an increase in quality of the post-processing images, as demonstrated in Fig. 1b-f. DSCT made scanning at a pitch >2 possible by filling the sampling gaps of one detector with data of the second detector, providing clinical advantages in (cardio)vascular, trauma and pediatric patients due to increased scan speed (Fig. 1f) [40,41].

4.7. Rotation time and temporal resolution

Gantry rotation time directly affects TR as data from at least a 180-degree rotation are needed to reconstruct an image. Faster gantry rotation times result in improved TR with less motion artifacts and improved clarity of lung and cardiac imaging [42,43]. Gantry rotation times have decreased from 5 to 40 seconds in rotation-translation systems in the seventies to 0.24−0.30 seconds for the current CT systems [26]. Until today, most single source scanners still cannot reach the 50–100 ms TR of electron beam CT scanners. Those scanners were especially proposed for cardiac CT because they were able to reach good TR thanks to its scanning without mechanical motion [44]. It was until the introduction of DSCT to achieve similar TR with up to 66 ms with 3rd generation CT systems [45].

4.8. Electrocardiogram (ECG) synchronization and ECG-guided dose modulation

Cardiac motion limited imaging of the heart in the early years of CT. However, in 1977 there were considerable achievements in technology reducing cardiac motion by ECG-gated reconstruction and provided "stop-action" cardiac CT scans [46,47]. However, acquiring data for a single slice took up to 12 s. Multi-detector spiral CT reduced exam time, enabled reducing contrast volume, improved spatial resolution and ECG-gated coronary CT angiography became feasible in clinical practice. Especially from the 64-row MDCT on, robust low heart rate (HR) cardiac CT was possible (Fig. 1e). [48,49]. At first, only a retrospective spiral scan mode with full dose, during the whole R-R interval at low pitch values was provided [50]. Later on, by introducing adaptive algorithms which can react to heart rate variability and simple arrhythmia, a dose reduction was achieved [51]. When the heart rhythm has complex arrhythmia, often a retrospective protocol is preferred for ECG gated data editing possibilities. However, such a protocol requires a low pitch for oversampling to ensure enough data for reconstruction is available at the expense of a high(er) radiation dose. While a prospective sequential scanning technique might have stack artifacts, a single heart beat scan mode such as a high-pitch prospective scan or a scan with a wide area detector does not. However, both single heart beat techniques require a low and stable heart rate [52].

5. Reconstruction parameters

Some of the steps in the reconstruction process are not, or to a less degree, adjustable by the user. All of the choices made within the reconstruction process directly influence IQ. We will highlight the main technological developments in reconstruction techniques.

5.1. Image reconstruction technique

Within the first CT systems, images were reconstructed with a simple iterative reconstruction method known as algebraic reconstruction [53]. However, due to the lack of computing power, this technique was soon replaced by filtered backprojection (FBP) [54]. FBP images are reconstructed by a convolution method or a direct Fourier algorithm. This second group incorporated interpolation in the Fourier plane, followed by inverse Fourier transformation. Convoluting the attenuation profiles with a so-called kernel and the backprojection of the modified profiles into the image plane to create the final image, is the method known as filtered backprojection. It is an analytical solution of the reconstruction problem. Where FBP was the most widely used CT image reconstruction technique for decades, nowadays mainly IR techniques are applied [55].

5.1.1. Iterative reconstruction technique

Computing power by the late ’00 made IR techniques feasible in clinical routine [55]. IR techniques developed rapidly in three steps: Firstly, IR reconstruction was mainly done in the image domain on an initial image reconstructed from the raw data, secondly it went to sinogram-based or so-called hybrid reconstructions. Thirdly, reconstruction algorithms developed to full model-based IR techniques [56]. However, most algorithms remain a “black-box” lacking specific details.

5.2. Matrix and FoV

Within the first-generation CT scanners, the image matrix size was limited to 80×80 pixels and one could only adjust the window level and width. Nowadays 512×512 is the most commonly used image matrix size but CT scanners with sizes up to 2048×2048 are available [57].

Extended field of view (FoV) reconstructions allow visualization of skin and tissue outside the primary FoV. This is of importance for PET-CT attenuation correction and radiotherapy CT dose calculations [58].

5.3. Cardiac reconstructions

The multiple ECG cycles acquired for cardiac CT in the late seventies were needed for acceptable effective TR with the aid of multi-segment reconstruction. Despite long acquisition time and extensive motion artifacts, the cardiac outline and fat grooves could be sharply visualized. Nowadays, mono-segment reconstruction is often used, but bi- or multi-segment reconstruction techniques are still available to make scanning of coronaries at higher heartrates feasible. These methods could improve the TR by a factor of 2 by combining two or more heart beats for one reconstruction, but at the cost of a very low pitch value and consequently an increased radiation dose [50]. A disadvantage of multi-segment reconstruction is a possible creation of blurry images [59]. Even though vendors developed motion reduction algorithms, motion free imaging primarily depends on heart rate and gantry rotation time [60,61].

5.4. Image enhancement tools

Several tools to improve IQ are developed and can be manually selected or are integrated into the reconstruction process. The most often used tools are noise and artifact reduction algorithms.

5.5. Noise reduction

Recently, noise reduction algorithms are implemented in several reconstruction processes, mostly running in the background e.g. in repeated low dose imaging during dynamic CT perfusion, in order to improve spatial resolution and CNR [62]. Sometimes it can be manually applied by the user e.g. to improve CNR in monoenergetic image reconstruction of dual energy data [63].

5.6. Artifact reduction

Artifacts are defined as artificial structures, which deviate from reality. Examples are artifacts occurring from voluntary and involuntary patient motion or beamhardening. Nowadays, motion correction algorithms are often used in CT perfusion of the head and body to correct for subtle head displacement or the breathing state during the acquisition times. The corrections are applied on already reconstructed image data and mainly done in post-processing software. Whereas most of the algorithms for beam hardening correction or metal artifact reduction use iterative algorithms and therefore have to be applied on raw data [64].

6. Scanning protocol optimization

Technological developments generally resulted in a reduction of radiation dose per exam and improved IQ [65,66]. Both radiation dose and IQ are dictated by the ALARA (As Low as Reasonably Achievable) principle. With the introduction of diagnostic reference levels for CT in 1996, a practical tool came available to promote radiation dose optimization for specific diagnostic tasks [67]. With that, reference levels for CT exams were introduced around the globe [68–71]. Together with the technological developments it contributed to the decrease of effective dose for a CT exam [72]. However, the diagnostic reference levels are general guidelines and do not apply to optimization for an individual patient. In the meantime, the user is one of the “protocol optimization factors” or may be even the most important factor in the optimization process. The user’s contribution to the optimization process depends on the user himself and on the technological developments. All stakeholders, e.g. radiologist, medical physicist, and radiographer should work together and consider the whole optimization process as a team effort. In the next paragraph we will discuss the optimization process. Some optimization steps are highlighted by a single case study (Fig. 2), which covers a wide area of technological developments over more than a decade. Note: As there are several CT manufacturers, so are (subtle) differences in their approaches in the technological developments in system, acquisition, and reconstruction parameters. Generalizations should come in only if features are significantly similar in all or most common vendors.

The whole scan protocol optimization process strives for optimization for an individual patient, taking the specific organ region and the referral question into account. Some technological developments have a direct effect on radiation dose applied to a patient (e.g. tube current). Other developments, like iterative reconstructions or automatic adaptation of tube voltage, are dependent on the user’s motivation, acceptation and awareness. Benefits of the increased and evolved technologies are known, but the technological developments were and could be misunderstood or misused, leading to excessive radiation dose to the patient [73,74]. Thereby, awareness of radiation dose and the possible risks are not always known [75].

Within the optimization process, the user’s influence has increased, while automated tools were integrated to assist in the optimization process. This does not mean that changing a parameter will lead to an automatic compensation in other features/parameters, for example to maintain image quality. Many of the acquisition and reconstruction

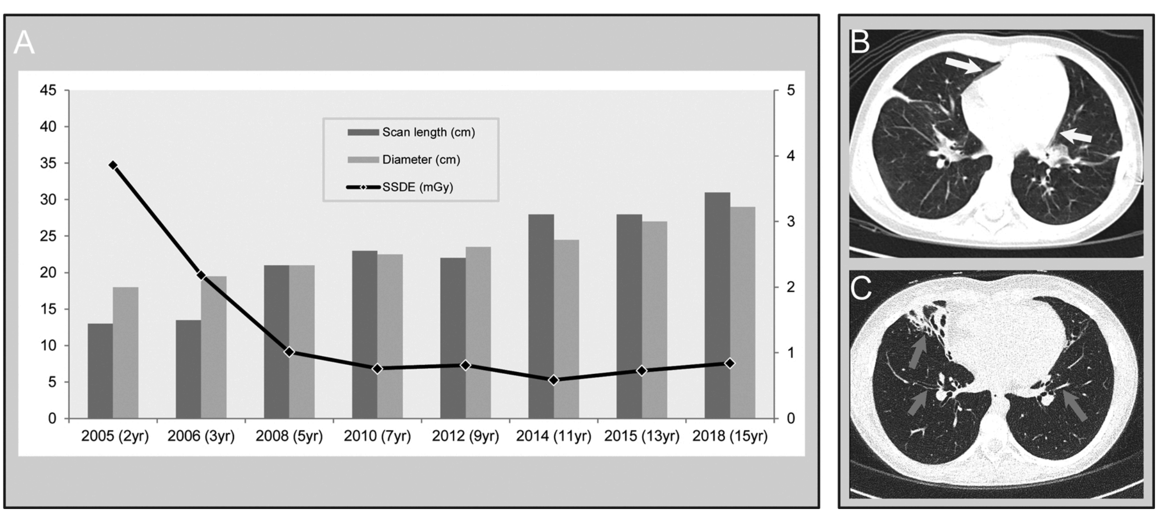

Fig. 2. (a-c) Case presentation of a female child in the follow-up of cystic fibrosis. **(a)** Scan length and the chest diameter are shown as vertical bars on the left y-axis. The size-specific dose estimates (SSDE) are illustrated as diamonds on the secondary, right y-axis. At first, the patient was scanned with anesthesia on a 6-slice CT scanner with a slice width of 2.5 mm within the period 2005 – 2008. Tube voltage was fixed in this period and the scans in 2006 and 2008 were performed with a technician controlled breath hold. **(b)**. From 2010 – 2018, the patient was scanned with spirometry controlled breath hold on dual source CT, equipped with faster rotation time and thinner detector collimation. Within this period, scan protocol was optimized with iterative reconstruction technique, automatic tube voltage selection, and additional tin filtration. **(c)** CT scan (axial view) of the chest (2018) diameter increased from 18 cm to 29 cm and the scan length increased accordingly from 13 cm to 31 cm. SSDE dropped with almost 80 %. Image noise was increased between **(b)** and **(c)** while increasing image quality due to improved temporal resolution and spatial resolution: White arrows in **(b)** show motion artifacts and the grey arrows in **(c)** show sharp delineation of the lung vessels and the airway wall.

parameters are interrelated, making them more complicated to adjust individually and more difficult to comprehend, especially when they are part of automated algorithms and, likely, in the near future with artificial intelligence. Nevertheless, technological improvements and automated tools, combined with attention to the human side by the radiographer, will lead to the optimal scanning procedure. For example, automatization might speed up the scanning and reconstruction process, while the main focus of the radiographer is on the patient itself. In the meantime, adjusting parameters is like slotted dials: On the road to optimization, regardless of whether the adjustments have been made by humans or artificial intelligence, an adjustment of an acquisition or reconstruction parameter will have a direct influence on image quality and, directly or indirectly, on radiation dose as well due to their interrelation (Fig. 3). Within this light, it is mandatory to focus first on diagnostic optimization, which can be defined, and achieved, by the determination of the minimally acceptable IQ for diagnosis and thus of the lower limit of the diagnostic reference level. Minimally acceptable IQ is set by the desired image contrast, spatial resolution, and the amount of artifacts accepted [76,77]. The second step will be technological optimization, defined as parameter selection to achieve this preferred lower limit IQ at the lowest reasonable dose. Fig. 2 shows an example how a thoracic scanning protocol was technologically optimized. Users should be aware that diagnostic and technological optimization outcomes may vary between different CT scanners and institutions with different IQ preferences [71,78]. The impact of a change in acquisition and reconstruction parameters on IQ and radiation dose, together with considerations for protocol optimization is illustrated in Table 2. This table is used as a guidance for the next paragraphs to discuss the impact of adaptation of a single parameter on IQ and radiation dose.

6.1. Acquisition parameters

Protocol optimization for every individual patient can be obtained by adaptation of a single or multiple acquisition parameters. Every parameter demands its own consideration for optimization (Table 2, “considerations for CT protocol optimization”). For instance, when objects have slight attenuation differences such as in soft tissue studies, image noise impairs contrast resolution. So again, it is essential to determine the tolerance level of noise in the CT images as Sir Hounsfield already stated in 1976 [79]. An increase in noise is not problematic in objects with high intrinsic contrast, e.g. bone and air ways. [57,79].

Adaptation of the tube voltage will have different effects and depends on whether or not iodinated contrast material is used (Table 2, “acquisition parameters”, “image quality”, “radiation dose”) and on the general strategy for using automatic tube voltage selection [80]. X-ray attenuation by objects such as bone and iodine contrast strongly depends on the photon energy due to their high atomic number. Therefore, when iodine material is used, an improved CNR is possible, e.g. to better depict enhancing masses, at a low tube voltage with a dose similar to a high tube voltage scan (Fig. 4AB) [81]. On the other hand, for scanning protocol optimization in e.g. young patients, the user may consider a reduction of radiation dose while maintaining CNR (Fig. 4C) [82]. While the main goal of automatic tube voltage selection is to control the CNR and thereby minimize radiation dose, sometimes the user should adjust the proposed parameters by the scanner software for an individual patient, instead of following the general strategy for automatic tube voltage selection. Thus, in some cases the referral question or individual patient demands for a higher radiation dose. For example, the user may also want to apply a higher contrast volume or flow since a high tube voltage decreases iodine contrast enhancement (Fig. 5AB).

The presence of high attenuating materials such as a hip prosthesis (Fig. 5CD), warrants an increased tube voltage to decrease artifacts when no metal artifact reduction techniques are available (Table 2, “risk of artifacts”).

Continuing with the parameter adaptation shown in Table 2: In general, tube current adaptation is not dependent on the use of iodine material, but rather on the noise tolerated in the images. Modulation of the tube current is used throughout most of the CT scanning protocols. Its use changes the relative dependencies in individual exposure parameters. For example, changing the pitch or rotation time often does not affect the patient’s dose, as a change in tube current compensates for the change in other parameters [83]. However, when using ATCM, one should be aware that specific parameters, like slice thickness, kernel, and tube voltage, may affect the behavior of ATCM and that this differs between vendors [84].

Considerations to increase TR and the pitch mostly depend on the need of decreasing motion artifacts (Fig. 2B and 2C), mainly when

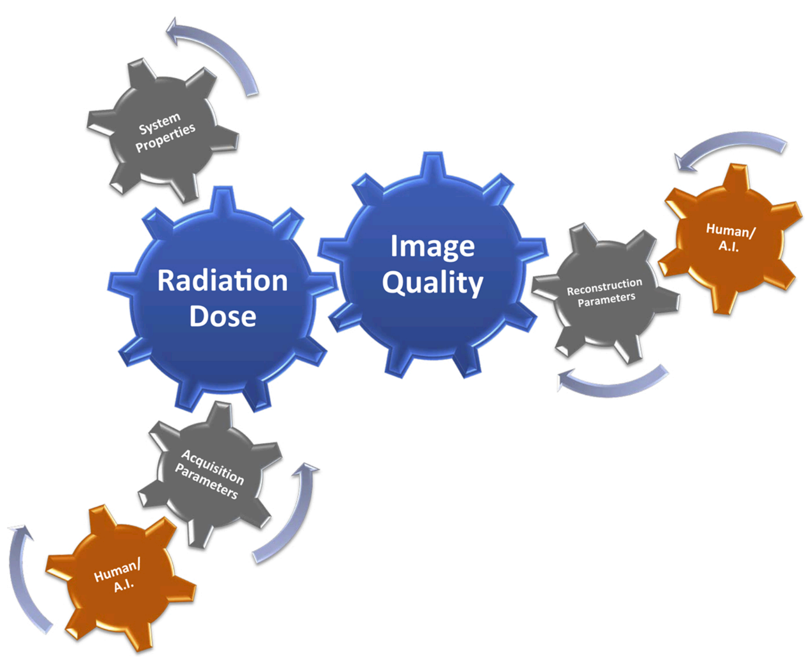

Fig. 3. Graphical illustration by slotted dials, demonstrating the balance between optimization of a scanning protocol with respect to image quality and radiation dose. Changing system properties or parameters, input of human or artificial intelligence will influence both radiation dose and image quality.

Table 2
Overview of general impact when adapting acquisition and reconstruction parameters currently used.

Acquisition Parameters	Image Quality			Radiation Dose Direct Absolute Effect	Considerations for CT Protocol Optimization
	Contrast Resolution	Spatial Resolution	Risk of Artifacts		
Tube current increase	+	≈	≈	+ (linear)	Increase of contrast resolution and decrease of noise at the cost of increased radiation dose
Tube current decrease	−	≈	≈	− (linear)	Decrease of radiation dose at the cost of decrease of contrast resolution and increase of noise
Tube voltage increase (no iodinated contrast material applied)	soft tissue ≈ / − bone/fat	≈	− (1,2)	+ (non-linear)	Decrease of artifacts and noise at the cost of increased radiation dose and decreased contrast of bone/fat
Tube voltage decrease (no iodinated contrast material applied)	soft tissue ≈ / + bone/fat	≈	+ (1,2)	− (non-linear)	Increase of contrast bone/fat and decreased radiation dose at the cost of increase of artifacts and noise
Tube voltage increase (iodinated tissue)	soft tissue − / − bone/fat	≈	− (1,2)	+ (non-linear)	Decrease of artifacts and noise at the cost of increased radiation dose and decreased contrast of bone/fat, especially soft tissue (iodine)
Tube voltage decrease (iodinated tissue)	soft tissue ++ / + bone/fat	≈	+ (1,2)	− (non-linear)	Increase of contrast in soft tissue (iodine) and bone/fat with decreased radiation dose at the cost of increase of artifacts and noise
Sequential/ Axial (relative to spiral)	≈	−	− (3) / + (4)	− (non-linear)	No windmill/spiral artifacts and no overranging dose at the cost of increased stair-step artifacts and impaired scan speed
Multi-detector spiral (relative to sequential)	≈	+	+ (3) / − (4)	+ (linear)	Increased spatial resolution and scan speed at the cost of overranging dose and possible windmill/spiral artifacts
Pitch increase	−	−	+ (3) / − (5)	−	Decrease of motion artifacts, increase windmill/ spiral artifacts. Increase of noise when keeping tube current constant (strategies vary between vendors): Absorbed dose decrease. Overranging dose increase, but depends on the beam collimation, scanning range and the presence of dynamic collimation
Pitch decrease	+	+	- (3) / + (5)	+	Increase of motion artifacts, but decrease of noise and windmill/spiral artifacts and increase of contrast and spatial resolution. Increase of absorbed dose due to constant tube current (strategies may vary between vendors) and a decrease of overranging dose. Overranging depends on beam collimation and the presence of dynamic collimation as well.
Longer rotation time	+	+ / ++ (a)	− (3,6) / ++ (5)	+ (linear)	Increase of contrast and spatial resolution with decrease of windmill/ spiral artifacts with active flying focal spot and decrease of blooming at the cost of increased motion artifacts and radiation dose
Shorter rotation time	−	− / ≈ (a)	+ (3,6) / −− (5)	- (linear)	Decrease of motion artifacts and reduced radiation dose at the cost of increased windmill/spiral artifacts when no active flying focal spot is used, increase of blooming and noise with decreased contrast and spatial resolution
Reconstruction Parameters	Image Quality			Radiation Dose Direct Absolute Effect	Considerations for CT Protocol Optimization
	Contrast Resolution	Spatial Resolution	Risk of Artifacts		
Iterative reconstruction technique (relative to filtered back-projection)	+	≈ / + (model based)	≈ / − (model based)	≈	Increase of contrast and spatial resolution with ability to reduce radiation dose and artifacts; probably user adaptation to different image impression
Matrix increase	−	+	− (6)	≈	Increase of spatial resolution; necessity to increase radiation dose to preserve the same SNR
Matrix decrease	+	−	+ (6)	≈	Increase of contrast resolution but increase of partial volume effect; ability to reduce radiation dose
dFoV increase	+	−	+ (6)	≈	Increase of contrast resolution but increase of partial volume effect; ability to reduce radiation dose
dFoV decrease	−	+	− (6)	≈	Increase of spatial resolution; necessity to increase radiation dose to preserve the same SNR
Slice thickness increase	+	−	− (3) / + (6)	≈	Increase of contrast resolution but increase of partial volume effect; ability to reduce radiation dose and windmill/spiral artifacts
Slice thickness decrease	−	+	− (6)	≈	Increase of spatial resolution with decrease of partial volume effect; necessity to increase radiation dose to preserve the same SNR

Note. : Increase is demonstrated with the "+", decrease with the "−", and (almost) equal effect with the "≈". dFoV = display field of view. Data in paranthesis 1=beamhardening; 2=streak; 3=windmill/spiral; 4=stair-step; 5=motion/breathing/pulsation; 6=partial volume effect/ blooming; a=active flying focal spot.

imaging the heart or scanning non-cooperative patients. However, a higher pitch value often demands a higher tube current, especially in scanners that keep the noise and dose level constant. Faster rotation times may increase artifacts. Therefore, in cases of cooperative patients, the user may decrease the pitch to decrease the overranging effect. Moreover, this will also lead to increased IQ in e.g. bone exams, especially when the structures are angulated relative to scan plane [18,85].

6.2. Reconstruction parameters

CT protocol optimization is also obtained by adaptation of single, or multiple, reconstruction parameters (Table 2). In image reconstruction, when selecting the level of smoothing (minimal, moderate, or maximum), the user can improve low contrast detectability by reducing the amount of noise. The other way around, edge-enhancement filters improve spatial resolution, by "sharpening up" the CT image and are especially useful in bone or lung exams [86]. Other filters may increase

Fig. 4. (a-c) Axial CT images of the same human abdomen acquired with equal CTDIvol and contrast injection protocol. Window width and level were 300/30. Images made with two days in between. **(a)** Demonstrating an increased contrast to noise ratio (CNR) when applying a lower tube voltage of 80 kVp compared to the CNR observed in **(b)** with 120 kVp. **(c)** CT image (maximum intensity projection, coronal view) of the heart of a thirteen-year-old boy. Reduced radiation dose in coronary CT angiography when applying low tube voltage (70 kV, a total dose length product of 8.2 mGy*cm, and a SSDE of 0.77 mGy).

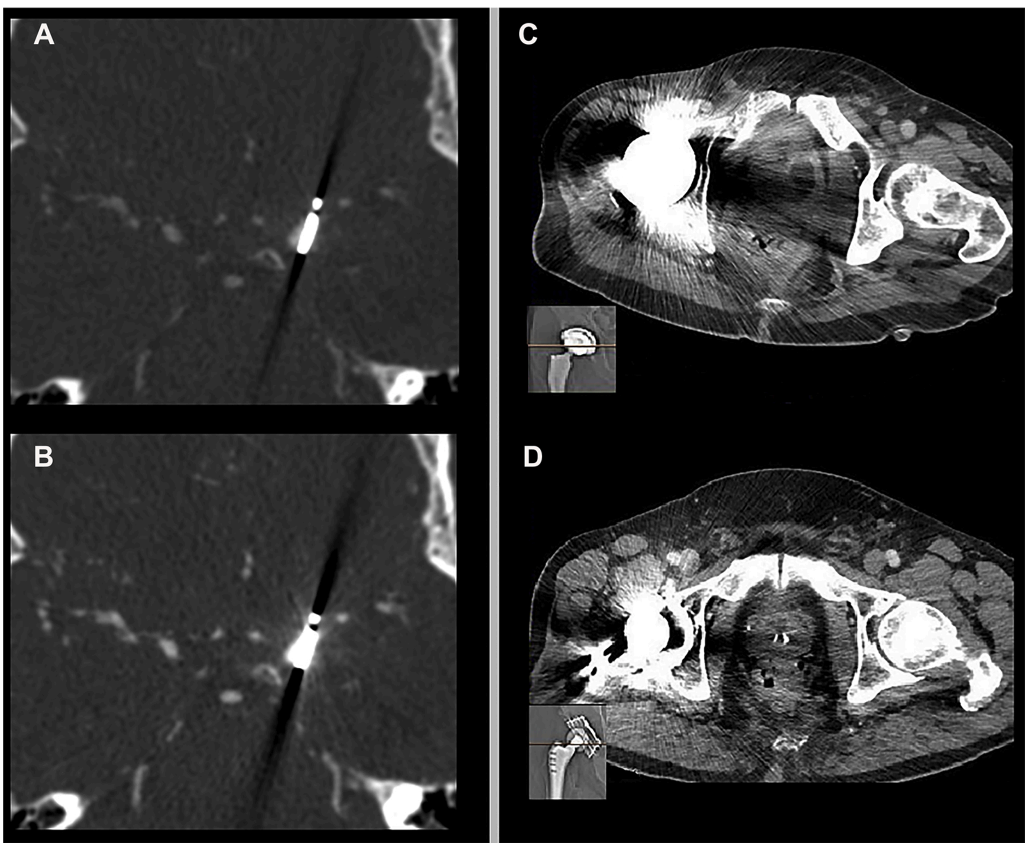

Fig. 5. (a-d) Axial CT images demonstrating the influence of adjusting the tube voltage on metal artifacts and image quality in contrast enhanced CT scans. **(a-b)** Dual energy CT angiography of a clipped brain aneurysm with metal clip artifacts **(a)** 140 kV scan with low contrast HU, but with less beam hardening artifacts than in **(b)** 80 kV scan with high contrast HU. **(c-d)** CT of the abdomen of two different patients with hip prosthesis **(c)** Hip prosthesis with cobalt head causing disturbing beam hardening artifacts in the pelvic area. Not all metal type will cause disturbing beam hardening: **(d)** Hip prosthesis with a head made of titanium and a clear visualization of the pelvic area.

metal to tissue transition such as stent lumen by reducing blooming effects [87]. An improved spatial resolution comes with an increased noise level and reduced soft tissue contrast.

Within iterative reconstruction techniques, careful considerations in iterative strength, also known as level or scale, and accompanied dose adjustments are mandatory [88,89]. For instance, higher iterative strength can have an effect on contrast and spatial resolution, but also on image appearance [90]. The image texture might be blurred and a high iterative strength can give rise to a noiseless image appearance. These kind of images are often evaluated as too smooth or artificial, neither are often desired by users [91]. Reliable diagnostic quality and statistically significant dose reductions can be achieved in adult and pediatric patients using IR [92,93]. However, negative effects as low contrast detectability are reported as well [94].

Spatial resolution may increase with increased matrix size thanks to a decrease of the voxel size. In general this will be accompanied by an increase of noise (Table 2). Moreover, users should also be aware that image data size increases with increased matrix size.

Adaptation of the FoV is also related to the voxel size: Increasing or decreasing the FoV will directly influence voxel size. Thereby, it may affect IQ: a smaller FoV may increase spatial resolution, but decrease contrast resolution due to increase of noise. Balancing between optimization of a protocol with respect to IQ and radiation dose, e.g. the increase of spatial resolution, at the cost of image noise, the user may also want to adjust the slice thickness to restore the signal-to-noise ratio. For example, when an increase in contrast resolution is required, noise levels can be lowered by increasing slice thickness (Fig. 6AB). Simultaneously, spatial resolution will decrease due to the partial-volume effect (Fig. 6CD).

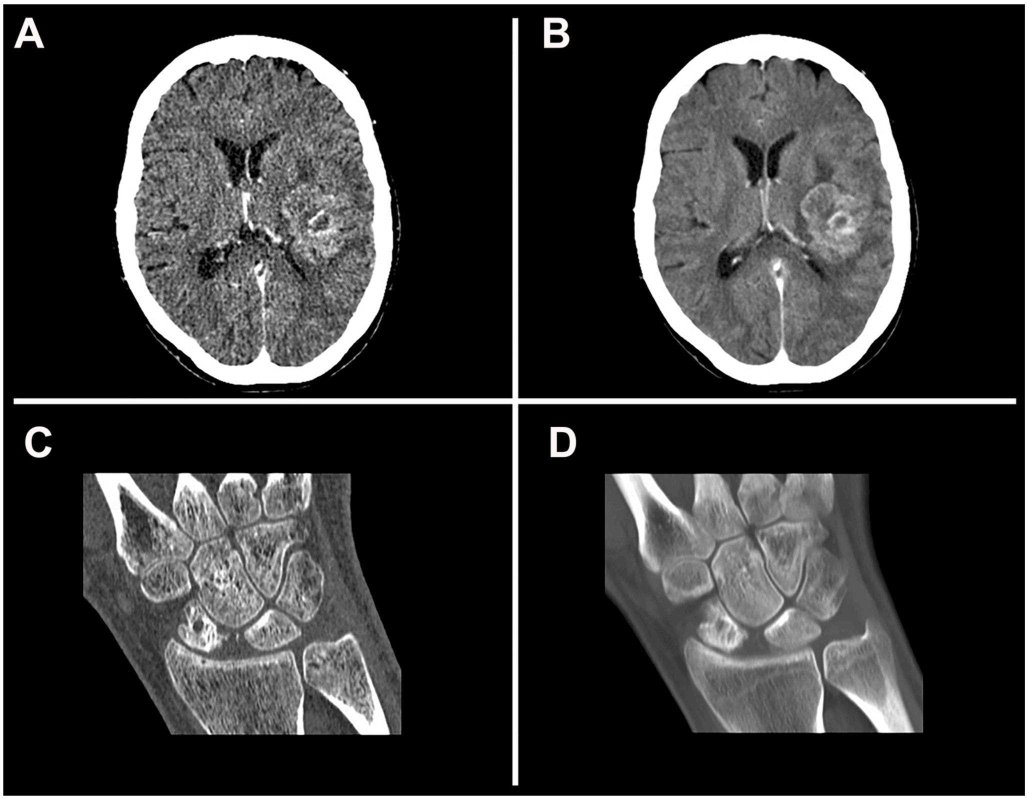

Fig. 6. (a-d) CT images illustrating the influence of adjusting a reconstruction parameter (slice thickness) and its influence on contrast and spatial resolution. **(a-b)** CT images (axial view) of an adult brain (soft tissue) **(a)** 1.0 mm and **b** 5.0 mm. **(c-d)** CT images (multiplanar reconstruction, coronal view) of a wrist (bone). Contrast resolution is increased with thicker slices due to decrease of noise. **(c)** 0.75 mm and **(d)** 5.0 mm. Spatial resolution is increased with thinner slices due to decrease of the partial volume effect.

7. Future outlook and conclusion

CT is still evolving, even in its middle age, and bringing new technological developments and new diagnostic strategies for healthcare. Users should not only be at the forefront in embracing latest technologies, but also be proactive on the road to highly optimized protocols.

Currently, photon counting CT (PCCT) and artificial intelligence (AI) promise to bring a new revolution in CT [55,72] (Fig. 1g). PCCT is expected to provide intrinsic spectral sensitivity, high spatial resolution, less noise and artifacts with better low-signal performance, and less characteristic energy-weighting [55,95]. PCCT opens the possibility of achieving multi-energy imaging in every scan, similar to dual energy CT, but using a single tube voltage. Where dual layer CT uses a single tube voltage too, PCCT is able to count the number of all incoming photons and measure its energy. Improved iodine contrast visibility may even require less radiation dose, or lower iodine contrast material injection [96,97].

AI is already applied within clinical protocols for instance in artifact reduction and image reconstruction [95]. As such the application of AI resembles IR: its application can be used to reduce radiation dose while maintaining IQ or increase IQ without increasing radiation exposure [55]. Both PCCT and AI are one of the latest technological developments in almost five decades of CT, but certainly will not be the last to be introduced and demanding an adjustment of the optimization process.

In conclusion, technological developments in CT have led to an increased number of processes for protocol optimization. Consequently, it is necessary that users are aware of those developments, their operation, and how they are interrelated with respect to image quality and radiation dose.

Guarantor

The scientific guarantor of this publication is Marcel van Straten

Statistics and biometry

One of the authors has significant statistical expertise.

Informed consent

Written informed consent was not required for this study because this concerns a narrative review paper.

Ethical approval

Institutional Review Board approval was not required because this concerns a narrative review paper.

Methodology

Narrative review paper

Funding

The authors state that this work has not received any funding.

Declaration of Competing Interest

R. Booij: Research collaboration, Siemens Healthineers
R.P.J. Budde: None
M.L. Dijkshoorn: Clinical training consultant: Siemens Healthineers
M. van Straten: Research collaboration, Siemens Healthineers

Our department has a Master Research Agreement with Siemens Healthineers. No funding or financial support was received for preparation of this article.

Acknowledgements

We would like to thank Dr. Wichor Bramer of the medical library

Erasmus MC for his support in building the search syntax.

Appendix A. Supplementary data

Supplementary material related to this article can be found, in the online version, at doi:https://doi.org/10.1016/j.ejrad.2020.109261.

References

[1] G.D. Rubin, Computed tomography: revolutionizing the practice of medicine for 40 years, Radiology 273 (2 Suppl) (2014) S45–74.
[2] D.J. Brenner, E.J. Hall, Computed tomography–an increasing source of radiation exposure, N. Engl. J. Med. 357 (22) (2007) 2277–2284.
[3] J.M. Meulepas, C.M. Ronckers, A. Smets, R.A.J. Nievelstein, P. Gradowska, C. Lee, A. Jahnen, M. van Straten, M.Y. de Wit, B. Zonnenberg, W.M. Klein, J.H. Merks, O. Visser, F.E. van Leeuwen, M. Hauptmann, Radiation exposure from pediatric CT scans and subsequent Cancer risk in the Netherlands, J. Natl. Cancer Inst. 111 (3) (2019) 256–263.
[4] M. Bosch de Basea, J.A. Salotti, M.S. Pearce, J. Muchart, L. Riera, I. Barber, S. Pedraza, M. Pardina, A. Capdevila, A. Espinosa, E. Cardis, Trends and patterns in the use of computed tomography in children and young adults in Catalonia - results from the EPI-CT study, Pediatr. Radiol. 46 (1) (2016) 119–129.
[5] W.A. Kalender, Dose in x-ray computed tomography, Phys. Med. Biol. 59 (3) (2014) R129–50.
[6] A. Kaul, B. Bauer, J. Bernhardt, D. Nosske, R. Veit, Effective doses to members of the public from the diagnostic application of ionizing radiation in Germany, Eur. Radiol. 7 (7) (1997) 1127–1132.
[7] L.T. Dauer, R.H. Thornton, J.L. Hay, R. Balter, M.J. Williamson, J. St Germain, Fears, feelings, and facts: interactively communicating benefits and risks of medical radiation with patients, AJR Am. J. Roentgenol. 196 (4) (2011) 756–761.
[8] S.P. Power, F. Moloney, M. Twomey, K. James, O.J.O.' Connor, M.M. Maher, Computed tomography and patient risk: facts, perceptions and uncertainties, World J. Radiol. 8 (12) (2016) 902–915.
[9] G.N. Hounsfield, Computed medical imaging. Nobel lecture, Decemberr 8, 1979, J. Comput. Assist. Tomogr. 4 (5) (1980) 665–674.
[10] W.A. Kalender, X-ray computed tomography, Phys. Med. Biol. 51 (13) (2006) R29–43.
[11] J. Ambrose, Computerized transverse axial scanning (tomography): Part 2. Clinical application, Br. J. Radiol. 46 (552) (1973) 1023–1047.
[12] G.N. Hounsfield, The E.M.I. scanner, proceedings of the royal society of london, Series B. Biol. Sci. 195 (1119) (1977) 281.
[13] H. Takagi, R. Tanaka, K. Nagata, R. Ninomiya, K. Arakita, J.D. Schuijf, K. Yoshioka, Diagnostic performance of coronary CT angiography with ultra-high-resolution CT: comparison with invasive coronary angiography, Eur. J. Radiol. 101 (2018) 30–37.
[14] W.A. Kalender, Computed Tomography - Fundamentals, System Technology, Image Quality, Applications, 3rd revised ed., Publicis Publishing, Erlangen, 2011.
[15] R. Klingebiel, E. Siebert, S. Diekmann, E. Wiener, F. Masuhr, M. Wagner, H. C. Bauknecht, M. Dewey, G. Bohner, 4-D Imaging in cerebrovascular disorders by using 320-slice CT: feasibility and preliminary clinical experience, Acad. Radiol. 16 (2) (2009) 123–129.
[16] F.J. Rybicki, H.J. Otero, M.L. Steigner, G. Vorobiof, L. Nallamshetty, D. Mitsouras, H. Ersoy, R.T. Mather, P.F. Judy, T. Cai, K. Coyner, K. Schultz, A.G. Whitmore, M. F. Di Carli, Initial evaluation of coronary images from 320-detector row computed tomography, Int. J. Cardiovasc. Imaging 24 (5) (2008) 535–546.
[17] I.A. Tsalafoutas, The impact of overscan on patient dose with first generation multislice CT scanners, Phys. Med. 27 (2) (2011) 69–74.
[18] R. Booij, M.L. Dijkshoorn, M. van Straten, Efficacy of a dynamic collimator for overranging dose reduction in a second- and third-generation dual source CT scanner, Eur. Radiol. 27 (9) (2017) 3618–3624.
[19] A. Altman, R. Carmi, TU-e-210A-03: a double-layer detector, dual-energy CT — principles, advantages and applications, Med. Phys. 36 (6Part24) (2009), 2750-2750.
[20] R. Homberg, R. Koeppel, An X-ray tube assembly with rotating anode spiral groove bearing of the 2nd generation, Electromedica 66 (2) (1997) 65–66.
[21] Y. Kyriakou, M. Kachelriess, M. Knaup, J.U. Krause, W.A. Kalender, Impact of the z-flying focal spot on resolution and artifact behavior for a 64-slice spiral CT scanner, Eur. Radiol. 16 (6) (2006) 1206–1215.
[22] S. Gordic, F. Morsbach, B. Schmidt, T. Allmendinger, T. Flohr, D. Husarik, S. Baumueller, R. Raupach, P. Stolzmann, S. Leschka, T. Frauenfelder, H. Alkadhi, Ultralow-dose chest computed tomography for pulmonary nodule detection: first performance evaluation of single energy scanning with spectral shaping, Invest. Radiol. 49 (7) (2014) 465–473.
[23] M.S. May, M. Brand, M.M. Lell, M. Sedlmair, T. Allmendinger, M. Uder, W. Wuest, Radiation dose reduction in parasinus CT by spectral shaping, Neuroradiology 59 (2) (2017) 169–176.
[24] R.A. Robb, E.A. Hoffman, L. Sinak, L.D. Harris, E.L. Ritman, High-speed three-dimensional X-ray computed tomography: the dynamic spatial reconstructor, Proc. Ieee 71 (1983) 308–319.
[25] T.G. Flohr, C.H. McCollough, H. Bruder, M. Petersilka, K. Gruber, C. Suss, M. Grasruck, K. Stierstorfer, B. Krauss, R. Raupach, A.N. Primak, A. Kuttner, S. Achenbach, C. Becker, A. Kopp, B.M. Ohnesorge, First performance evaluation of a dual-source CT (DSCT) system, Eur. Radiol. 16 (2) (2006) 256–268.
[26] R. Gould, Early Days of CT: Innovations (Both Good and Bad), 51st AAPM Annual Meeting, 2009 (Accessed Available from https://www.aapm.org/meetings/amos2/pdf/42-12236-29343-41.pdf, accessed on 08-08-2018.
[27] G. Cohen, Contrast–detail–dose analysis of six different computed tomographic scanners, J. Comput. Assist. Tomogr. 3 (2) (1979) 197–203.
[28] W.A. Kalender, H. Wolf, C. Suess, M. Gies, H. Greess, W.A. Bautz, Dose reduction in CT by on-line tube current control: principles and validation on phantoms and cadavers, Eur. Radiol. 9 (2) (1999) 323–328.
[29] S. Ulzheimer, H. Endt, T. Flohr, Computed tomography-patient dose and dose reduction technologies, Health Phys. 100 (3) (2011) 325–328.
[30] T. Kaasalainen, K. Palmu, A. Lampinen, M. Kortesniemi, Effect of vertical positioning on organ dose, image noise and contrast in pediatric chest CT–phantom study, Pediatr. Radiol. 43 (6) (2013) 673–684.
[31] T. Toth, Z. Ge, M.P. Daly, The influence of patient centering on CT dose and image noise, Med. Phys. 34 (7) (2007) 3093–3101.
[32] L.M. Zatz, Image quality in cranial computed tomography, J. Comput. Assist. Tomogr. 2 (3) (1978) 336–346.
[33] F.C. Southon, CT scanner comparison, Med. Phys. 8 (1) (1981) i-i.
[34] J.C. Ramirez-Giraldo, M. Fuld, K. Grant, A.N. Primak, T. Flohr, New approaches to reduce radiation while maintaining image quality in multi-detector-Computed tomography, Curr. Radiol. Rep. 3 (2) (2015).
[35] T.R.C. Johnson, B. Krauß, M. Sedlmair, M. Grasruck, H. Bruder, D. Morhard, C. Fink, S. Weckbach, M. Lenhard, B. Schmidt, T. Flohr, M.F. Reiser, C.R. Becker, Material differentiation by dual energy CT: initial experience, Eur. Radiol. 17 (6) (2007) 1510–1517.
[36] W. Marshall, E. Hall, A. Doost-Hoseini, R. Alvarez, A. Macovski, D. Cassel, An implementation of dual energy CT scanning, J. Comput. Assist. Tomogr. 8 (4) (1984) 745–749.
[37] I.P. Almeida, L.E. Schyns, M.C. Ollers, W. van Elmpt, K. Parodi, G. Landry, F. Verhaegen, Dual-energy CT quantitative imaging: a comparison study between twin-beam and dual-source CT scanners, Med. Phys. 44 (1) (2017) 171–179.
[38] W.A. Kalender, Principles and applications of spiral CT, Nucl. Med. Biol. 21 (5) (1994) 693–699.
[39] W.A. Kalender, P. Vock, A. Polacin, M. Soucek, [Spiral-CT: a new technique for volumetric scans. I. Basic principles and methodology], Rontgenpraxis 43 (9) (1990) 323–330.
[40] S. Achenbach, M. Marwan, T. Schepis, T. Pflederer, H. Bruder, T. Allmendinger, M. Petersilka, K. Anders, M. Lell, A. Kuettner, D. Ropers, W.G. Daniel, T. Flohr, High-pitch spiral acquisition: a new scan mode for coronary CT angiography, J. Cardiovasc. Comput. Tomogr. 3 (2) (2009) 117–121.
[41] T.G. Flohr, S. Leng, L. Yu, T. Allmendinger, H. Bruder, M. Petersilka, C. D. Eusemann, K. Stierstorfer, B. Schmidt, C.H. McCollough, Dual-source spiral CT with pitch up to 3.2 and 75 ms temporal resolution: image reconstruction and assessment of image quality, Med. Phys. 36 (12) (2009) 5641–5653.
[42] G.D. Rubin, A.N. Leung, V.J. Robertson, P. Stark, Thoracic spiral CT: influence of subsecond gantry rotation on image quality, Radiology 208 (3) (1998) 771–776.
[43] M. Montaudon, P. Berger, H. Blachère, L. De Boucaud, V. Latrabe, F. Laurent, Thin-section CT of the lung: influence of 0.5-s gantry rotation and ECG triggering on image quality, Eur. Radiol. 11 (9) (2001) 1681–1687.
[44] D.P. Boyd, M.J. Lipton, Cardiac Computed Tomography, 1983.
[45] P.M. Carrascosa, R.C. Cury, M.J. García, J. Leipsic, Dual-Energy CT in Cardiovascular Imaging, Springer, 2015.
[46] G. Harell, D.F. Guthaner, R.S. Breiman, Stop-action cardiac computed tomography, Radiology 123 (1977) 515.
[47] S.S. Sagel, E.S. Weiss, R.G. Gillard, G.N. Hounsfield, G.T. Jost, R.J. Stanley, M. M. Ter-Pogossian, Gated computed tomography of the human heart, Invest. Radiol. 12 (6) (1977) 563–566.
[48] K. Nieman, M. Oudkerk, B.J. Rensing, P. van Ooijen, A. Munne, R.J. van Geuns, P. J. de Feyter, Coronary angiography with multi-slice computed tomography, Lancet 357 (9256) (2001) 599–603.
[49] M. Kachelrießs, S. Ulzheimer, W.A. Kalender, ECG-correlated image reconstruction from subsecond multi-slice spiral CT scans of the heart, Med. Phys. 27 (8) (2000) 1881–1902.
[50] T. Flohr, B. Ohnesorge, H. Bruder, K. Stierstorfer, J. Simon, C. Suess, S. Schaller, Image reconstruction and performance evaluation for ECG-gated spiral scanning with a 16-slice CT system, Med. Phys. 30 (10) (2003) 2650–2662.
[51] D.M.E. Bardo, P. Brown, Cardiac multidetector computed tomography: basic physics of image acquisition and clinical applications, Curr. Cardiol. Rev. 4 (3) (2008) 231–243.
[52] L.A. Neefjes, A. Rossi, T.S. Genders, K. Nieman, S.L. Papadopoulou, A. S. Dharampal, C.J. Schultz, A.C. Weustink, M.L. Dijkshoorn, G.J. Ten Kate, A. Dedic, M. van Straten, F. Cademartiri, M.G. Hunink, G.P. Krestin, P.J. de Feyter, N.R. Mollet, Diagnostic accuracy of 128-slice dual-source CT coronary angiography: a randomized comparison of different acquisition protocols, Eur. Radiol. 23 (3) (2013) 614–622.
[53] M. Beister, D. Kolditz, W.A. Kalender, Iterative reconstruction methods in X-ray CT, Phys. Med. 28 (2) (2012) 94–108.
[54] M.J. Willemink, P.A. De Jong, T. Leiner, L.M. De Heer, R.A.J. Nievelstein, R.P. J. Budde, A.M.R. Schilham, Iterative reconstruction techniques for computed tomography Part 1: technical principles, Eur. Radiol. 23 (6) (2013) 1623–1631.
[55] M.J. Willemink, P.B. Noel, The evolution of image reconstruction for CT-from filtered back projection to artificial intelligence, Eur. Radiol. (2018).
[56] K.W. Shaqdan, A.R. Kambadakone, P. Hahn, D.V. Sahani, Experience with iterative reconstruction techniques for abdominopelvic computed tomography in morbidly and super obese patients, J. Comput. Assisted Tomogr. 42 (1) (2018) 124–132.

[57] A. Hata, M. Yanagawa, O. Honda, N. Kikuchi, T. Miyata, S. Tsukagoshi, A. Uranishi, N. Tomiyama, Effect of Matrix Size on the Image Quality of Ultra-high-resolution CT of the Lung: Comparison of 512 × 512, 1024 × 1024, and 2048 × 2048, Acad. Radiol. 25 (7) (2018) 869–876.
[58] H. Bruder, M. Sedlmaier, K. Stierstorfer, T.G. Floh, High Definition Extended Field of View (HD FOV) Reconstruction in CT., RSNA (Radiological Society of North), Chicago, 2011.
[59] S.S. Halliburton, A.E. Stillman, T. Flohr, B. Ohnesorge, N. Obuchowski, M. Lieber, W. Karim, S.A. Kuzmiak, J.M. Kasper, R.D. White, Do segmented reconstruction algorithms for cardiac multi-slice computed tomography improve image quality? Herz 28 (1) (2003) 20–31.
[60] H. Schondube, T. Allmendinger, K. Stierstorfer, H. Bruder, T. Flohr, in: Evaluation of a Novel CT Image Reconstruction Algorithm With Enhanced Temporal Resolution, Medical Imaging 2011: Physics of Medical Imaging, Spie-Int Soc Optical Engineering, Bellingham, 2011.
[61] C. Rohkohl, H. Bruder, K. Stierstorfer, T. Flohr, Improving best-phase image quality in cardiac CT by motion correction with MAM optimization, Med. Phys. 40 (3) (2013).
[62] F. Pisana, T. Henzler, S. Schönberg, E. Klotz, B. Schmidt, M. Kachelrieß, Noise reduction and functional maps image quality improvement in dynamic CT perfusion using a new k-means clustering guided bilateral filter (KMGB), Med. Phys. 44 (7) (2017) 3464–3482.
[63] D. Marin, J.C. Ramirez-Giraldo, S. Gupta, W. Fu, S.S. Stinnett, A. Mileto, D. Bellini, B. Patel, E. Samei, R.C. Nelson, Effect of a noise-optimized second-generation monoenergetic algorithm on image noise and conspicuity of hypervascular liver tumors: an in vitro and in vivo study, Am J Roentgenol 206 (6) (2016) 1222–1232.
[64] R.H.H. Wellenberg, E.T. Hakvoort, C.H. Slump, M.F. Boomsma, M. Maas, G. J. Streekstra, Metal artifact reduction techniques in musculoskeletal CT-imaging, Eur. J. Radiol. 107 (2018) 60–69.
[65] A. Christe, J. Heverhagen, C. Ozdoba, C. Weisstanner, S. Ulzheimer, L. Ebner, CT dose and image quality in the last three scanner generations, World J. Radiol. 5 (11) (2013) 421–429.
[66] M.M. Rehani, Radiation protection in newer imaging technologies, Radiat. Prot. Dosim. 139 (1-3) (2010) 357–362.
[67] J.A. Brink, D.L. Miller, U.S. National diagnostic reference levels: closing the gap, Radiology 277 (1) (2015) 3–6.
[68] T.J. Boal, J.C. Hedt, P.F. Einsiedel, A survey of patient dose and image quality factors for CT scanners in Victoria, Australas. Phys. Eng. Sci. Med. 22 (3) (1999) 103–112.
[69] E.U. Ekpo, T. Adejoh, J.D. Akwo, O.C. Emeka, A.A. Modu, M. Abba, K.A. Adesina, D.O. Omiyi, U.H. Chiegwu, Diagnostic reference levels for common computed tomography (CT) examinations: results from the first Nigerian nationwide dose survey, J. Radiol. Prot. 38 (2) (2018) 525–535.
[70] D.D. Zhou, P. Sun, Z. Jia, W. Zhu, G. Shi, B. Kong, H. Wang, H. Zhang, Multisection computed tomography: results from a Chinese survey on radiation dose metrics, J. Chin. Med. Assoc. 82 (2) (2019) 155–160.
[71] P.C. Shrimpton, J.T. Jansen, J.D. Harrison, Updated estimates of typical effective doses for common CT examinations in the UK following the 2011 national review, Br. J. Radiol. 89 (1057) (2016) 20150346.
[72] C.H. McCollough, Computed tomography technology-and dose-in the 21st century, Health Phys. 116 (2) (2019) 157–162.
[73] W. Bogdanich, Radiation Overdoses Point up Dangers of CT Scans, New York Times website, 2009. www.nytimes.com/2009/10/16/us/16radiation.html.
[74] F.V. Coakley, R. Gould, B.M. Yeh, R.L. Arenson, CT radiation dose: what can you do right now in your practice? Am. J. Roentgenol. 196 (3) (2011) 619–625.
[75] I.L. Christoph, H.H. Andrew, P.M. Edward, A.B. James, P.F. Howard, Diagnostic CT Scans: Assessment of Patient, Physician, and Radiologist Awareness of Radiation Dose and Possible Risks, Radiology 231 (2) (2004) 393–398.
[76] L.W. Goldman, Principles of CT: radiation dose and image quality, J. Nucl. Med. Technol. 35 (4) (2007) 213–225.
[77] A. Jurik, J. Petersen, K.A. Jessen, G. Bongartz, J. Geleijns, S.J. Golding, M. Leonardi, E.V.P. Van Meerten, W. Panzer, P.C. Shrimpton, G. Tosi, Clinical use of image quality criteria in computed tomography: a pilot study, Radiat. Prot. Dosim. 90 (1-2) (2000) 47–52.
[78] European_Commission_Directorate-General_for_Energy, Radiation Protection N° 180: Medical Radiation Exposure of the European Population Part 1/2, EU Publications, 2015, https://doi.org/10.2833/708119. Available from, https://ec.europa.eu/energy/sites/ener/files/documents/RP180web.pdf.
[79] G.N. Hounsfield, Picture quality of computed tomography, Am. J. Roentgenol. 127 (1) (1976) 3–9.
[80] L. Yu, H. Li, J.G. Fletcher, C.H. McCollough, Automatic selection of tube potential for radiation dose reduction in CT: a general strategy, Med. Phys. 37 (1) (2010) 234–243.
[81] K. Tang, L. Wang, R. Li, J. Lin, X. Zheng, G. Cao, Effect of low tube voltage on image quality, radiation dose, and low-contrast detectability at abdominal multidetector CT: phantom study, J. Biomed. Biotechnol. 2012 (2012) 130169.
[82] R. Blankstein, M.A. Bolen, R. Pale, M.K. Murphy, A.B. Shah, H.G. Bezerra, A. Sarwar, I.S. Rogers, U. Hoffmann, S. Abbara, R.C. Cury, T.J. Brady, Use of 100 kV versus 120 kV in cardiac dual source computed tomography: effect on radiation dose and image quality, Int. J. Card. Imaging 27 (4) (2011) 579–586.
[83] M.K. Kalra, M.M. Maher, T.L. Toth, B. Schmidt, B.L. Westerman, H.T. Morgan, S. Saini, Techniques and applications of automatic tube current modulation for CT, Radiology 233 (3) (2004) 649–657.
[84] S. Sookpeng, C.J. Martin, D.J. Gentle, Investigation of the influence of image reconstruction filter and scan parameters on operation of automatic tube current modulation systems for different CT scanners, Radiat. Prot. Dosimetry 163 (4) (2015) 521–530.
[85] D.R. Ney, E.K. Fishman, D. Magid, D.D. Robertson, A. Kawashima, Three-dimensional volumetric display of CT data: effect of scan parameters upon image quality, J. Comput. Assist. Tomogr. 15 (5) (1991) 875–885.
[86] E.K. Fishman, D.R. Ney, A. Kawashima, W.W. Scott Jr, D.D. Robertson, Effect of image display on the quality of multiplanar reconstruction of computed tomography data, Invest. Radiol. 28 (2) (1993) 146–149.
[87] H. Seifarth, R. Raupach, S. Schaller, E.M. Fallenberg, T. Flohr, W. Heindel, R. Fischbach, D. Maintz, Assessment of coronary artery stents using 16-slice MDCT angiography: evaluation of a dedicated reconstruction kernel and a noise reduction filter, Eur. Radiol. 15 (4) (2005) 721–726.
[88] M.J. Willemink, T. Leiner, P.A. De Jong, L.M. De Heer, R.A.J. Nievelstein, A.M. R. Schilham, R.P.J. Budde, Iterative reconstruction techniques for computed tomography part 2: initial results in dose reduction and image quality, Eur. Radiol. 23 (6) (2013) 1632–1642.
[89] P.B. Noel, A.A. Fingerle, B. Renger, D. Munzel, E.J. Rummeny, M. Dobritz, Initial performance characterization of a clinical noise-suppressing reconstruction algorithm for MDCT, AJR Am. J. Roentgenol. 197 (6) (2011) 1404–1409.
[90] A. Winklehner, C. Karlo, G. Puippe, B. Schmidt, T. Flohr, R. Goetti, T. Pfammatter, T. Frauenfelder, H. Alkadhi, Raw data-based iterative reconstruction in body CTA: evaluation of radiation dose saving potential, Eur. Radiol. 21 (12) (2011) 2521–2526.
[91] O. Baskan, C. Erol, H. Ozbek, Y. Paksoy, Effect of radiation dose reduction on image quality in adult head CT with noise-suppressing reconstruction system with a 256 slice MDCT, J. Appl. Clin. Med. Phys. 16 (3) (2015) 5360.
[92] S. Singh, M.K. Kalra, A.S. Shenoy-Bhangle, A. Saini, D.A. Gervais, S.J. Westra, J. H. Thrall, Radiation dose reduction with hybrid iterative reconstruction for pediatric CT, Radiology 263 (2) (2012) 537–546.
[93] T.H. Wu, S.C. Hung, J.Y. Sun, C.J. Lin, C.H. Lin, C.F. Chiu, M.J. Liu, M.M.H. Teng, W.Y. Guo, C.Y. Chang, How far can the radiation dose be lowered in head CT with iterative reconstruction? Analysis of imaging quality and diagnostic accuracy, Eur. Radiol. 23 (9) (2013) 2612–2621.
[94] A. Mileto, L.S. Guimaraes, C.H. McCollough, J.G. Fletcher, L. Yu, State of the art in abdominal CT: the limits of iterative reconstruction algorithms, Radiology 293 (3) (2019) 491–503.
[95] M.M. Lell, M. Kachelrieß, Recent and Upcoming Technological Developments in Computed Tomography: High Speed, Low Dose, Deep Learning, Multienergy, Investigative Radiology Publish Ahead of Print (9000), 2020.
[96] Z. Yu, S. Leng, S. Kappler, K. Hahn, Z. Li, A.F. Halaweish, A. Henning, E.L. Ritman, C.H. McCollough, Low-dose Performance of a Whole-body Research Photon-counting CT Scanner, SPIE, 2016.
[97] A. Pourmorteza, R. Symons, D.S. Reich, M. Bagheri, T.E. Cork, S. Kappler, S. Ulzheimer, D.A. Bluemke, Photon-counting CT of the brain: in vivo human results and image-quality assessment, AJNR Am. J. Neuroradiol. 38 (12) (2017) 2257–2263.